



## OPEN ACCESS

EDITED BY  
Hien Nguyen,  
Vân Lang University, Vietnam

REVIEWED BY  
Sulaiman S. Alhudaithi,  
King Saud University, Saudi Arabia  
Moumita Dhara,  
Nitte College of Pharmaceutical Science,  
India

\*CORRESPONDENCE  
Guangchun Sun,  
✉ [sunguangchun@5thhospital.com](mailto:sunguangchun@5thhospital.com)

RECEIVED 04 December 2025  
REVISED 04 February 2026  
ACCEPTED 05 February 2026  
PUBLISHED 04 March 2026

CITATION  
Yang X, Sun G, Zhou X, Liang Q and Liu J  
(2026) Dual - functional cRGD/pH -  
sensitive liposomes loaded with sorafenib:  
a novel therapeutic approach for  
hepatocellular carcinoma.  
*Front. Nanotechnol.* 8:1760783.  
doi: 10.3389/fnano.2026.1760783

COPYRIGHT  
© 2026 Yang, Sun, Zhou, Liang and Liu.  
This is an open-access article distributed  
under the terms of the [Creative Commons  
Attribution License \(CC BY\)](https://creativecommons.org/licenses/by/4.0/). The use,  
distribution or reproduction in other  
forums is permitted, provided the original  
author(s) and the copyright owner(s) are  
credited and that the original publication  
in this journal is cited, in accordance with  
accepted academic practice. No use,  
distribution or reproduction is permitted  
which does not comply with these terms.

# Dual - functional cRGD/pH - sensitive liposomes loaded with sorafenib: a novel therapeutic approach for hepatocellular carcinoma

Xu Yang, Guangchun Sun\*, Xiaoyu Zhou, Qing Liang and Jing Liu

Department of Pharmacy, The Fifth People's Hospital of Shanghai, Fudan University, Shanghai, China

**Background:** Sorafenib, a first-line treatment for advanced hepatocellular carcinoma (HCC), is severely limited by its low oral bioavailability, lack of tumor specificity, and dose-limiting systemic adverse effects. Nanocarrier-based delivery systems, particularly liposomes, offer a promising strategy to overcome these limitations.

**Methods:** We developed a multifunctional liposomal system co-modified with a cyclic RGD (cRGD) peptide and pH-sensitive components (cholesteryl hemisuccinate, CHEMS) for sorafenib delivery (cRGD-pH-Lipo/Sor). The physicochemical properties, drug release profile, stability, and biosafety of this formulation were thoroughly characterized. Its targeting efficiency, cellular uptake, and antitumor efficacy were evaluated in both *in vitro* (Huh7 and HepG2 cells) and *in vivo* (Huh7-xenograft nude mice) models using techniques including HPLC, fluorescence imaging, CCK-8 and *in vivo* imaging system (IVIS).

**Results:** The optimized cRGD-pH-Lipo/Sor exhibited a uniform particle size distribution ( $116.73 \pm 1.07$  nm, polydispersity index of  $0.224 \pm 0.0017$ ), negative zeta potential ( $-22.2 \pm 3.50$  mV), high encapsulation efficiency (84.1%), and a desirable pH-responsive drug release profile (cumulative release: 73.2% at pH 5.0% vs. 38.4% at pH 7.4). *In vitro*, cRGD-pH-Lipo/Sor demonstrated significantly enhanced cellular uptake in HCC cells compared to free sorafenib and non-targeted liposomes, attributable to cRGD-mediated active targeting and pH-triggered release. *In vivo* imaging and biodistribution studies confirmed the superior tumor accumulation of cRGD-pH-Lipo. Most importantly, in a xenograft mouse model, cRGD-pH-Lipo/Sor achieved the most potent tumor growth inhibition without inducing significant systemic toxicity, as evidenced by body weight monitoring, serum biochemical analysis, and histopathological examination.

**Conclusion:** The cRGD-modified, pH-sensitive liposomal platform effectively addresses key pharmacological drawbacks of sorafenib. It enhances tumor-targeted delivery, promotes intracellular drug release, and significantly improves the therapeutic index, presenting a promising novel strategy for the systemic treatment of advanced HCC.

## KEYWORDS

CHEMS, cRGD peptide, HCC, liposome, sorafenib

## 1 Introduction

Hepatocellular carcinoma (HCC) represents a significant global health burden, ranking among the most prevalent digestive system malignancies, distinguished by its high morbidity and mortality rates (Vogel et al., 2022). The majority of patients are diagnosed at intermediate or advanced stages, where curative options like surgical resection, liver transplantation, or locoregional therapies are often no longer feasible (S et al., 2021; Chan et al., 2024). For decades, systemic therapy options for advanced HCC were severely limited and largely ineffective, contributing to its dismal prognosis. The landscape of systemic therapy for advanced HCC underwent a paradigm shift in 2007 with the approval of sorafenib, a multi-kinase inhibitor targeting vascular endothelial growth factor receptors (VEGFR), platelet-derived growth factor receptor (PDGFR), thereby inhibiting tumor cell proliferation and angiogenesis (Llovet et al., 2008). Landmark phase III clinical trials (SHARP and Asia-Pacific studies) initially demonstrated that sorafenib could prolong the median overall survival (OS) of patients with advanced HCC, and this survival benefit has been consistently validated in numerous subsequent clinical investigations (Cheng et al., 2009). Notably, sorafenib remained the unique first-line systemic therapy for advanced HCC until the advent of lenvatinib as an alternative first-line agent and the development of combination regimens such as atezolizumab plus bevacizumab (Cappuyns et al., 2025; Finn et al., 2020; Vogel et al., 2021).

Despite the expanding therapeutic landscape, sorafenib retains a vital role and provide a foundational and salvage treatment option for a significant proportion of the advanced HCC patient population, particularly for patients ineligible for or having progressed on immunotherapy-based regimens (Marrero et al., 2016; Gordan et al., 2024; Xie et al., 2023). Nevertheless, navigating its use presents significant clinical challenges, primarily dose-limiting toxicities and the rapid emergence of drug resistance. One major limitation is its low bioavailability. Sorafenib exhibits poor aqueous solubility and undergoes extensive first-pass metabolism, resulting in an absolute oral bioavailability of only 38%–49% in humans (Liu et al., 2016; Shukla et al., 2024; Ye H. et al., 2020), which significantly reduce the amount of drug available for systemic circulation and target tissue delivery. This erratic absorption leads to suboptimal and variable plasma concentrations, undermining dose-response predictability, and patients may not receive the full therapeutic benefits of sorafenib at standard doses.

Sorafenib's tumor selectivity is also suboptimal. As a multi-kinase inhibitor, it acts on a wide range of targets, but this lack of specificity may lead to off-target effects and limit its concentration at the tumor site (ElZayat et al., 2025; Escudier et al., 2019). Compared to tumor cells, normal tissues may also take up a significant amount of the drug, increasing the risk of side effects. These include hand-foot skin reaction (HFSR, 30%–60%), hypertension (17%–43%), diarrhea (30%–55%), and fatigue (15%–45%), frequently necessitating dose reduction or treatment interruption (Llovet et al., 2008; Llovet et al., 2018). These adverse reactions not only affect patients' quality of life but may also impact treatment adherence and outcomes. Ideally, a tumor-specific therapy should selectively target cancer cells while sparing normal tissues, but sorafenib's non-specific action partially undermines this goal.

Critically, these limitations form a vicious cycle: low oral bioavailability necessitates high-dose regimens to achieve therapeutic plasma concentrations, exacerbating off-target toxicities and compromising patient compliance. Concurrently, inadequate tumor accumulation diminishes the therapeutic index, precluding dose escalation. Consequently, over 70% of patients develop primary or acquired resistance within 6 months (Tang et al., 2020; Xia et al., 2020), underscoring an urgent need for strategies that enhance tumor-targeted delivery to overcome these pharmacological barriers.

To address these critical bottlenecks, liposomal nanocarrier drug delivery systems have emerged as transformative solutions, fundamentally revolutionizing drug bioavailability and tumor-targeted accumulation. The amphiphilic phospholipid bilayer (e.g., DSPC/Cholesterol) encapsulates hydrophobic therapeutics, transforming crystalline drugs into stable aqueous nanoformulations (Abu Lila and Ishida, 2017; Allen and Cullis, 2013; He et al., 2019). This structural design bypasses oral absorption barriers and abolishes first-pass-metabolism—key factors responsible for the low oral bioavailability of kinase inhibitors. However, conventional nanoscale drug delivery systems (NDDSs) face significant translational challenges, as their propensity for rapid phagocytosis and clearance by the reticuloendothelial system severely limits tumor tissue penetration (Barua and Mitragotri, 2014; Farjadian et al., 2019). While long-circulating NDDSs exhibit improved tumor accumulation, suboptimal intracellular distribution persists post-extravasation. This stems from inadequate cellular internalization efficiency, leading to premature drug release in the extracellular space. Compounding this issue, the absence of stimuli-responsive mechanisms impedes rapid drug deployment upon tumor arrival. Collectively, these limitations restrict the clinical utility of nanocarriers (Lee and Thompson, 2017; Perche and Torchilin, 2013; Hossen et al., 2019). Consequently, achieving both effective tumor-site accumulation and triggered intracellular drug release constitutes the dual challenge in developing high-efficacy anticancer nanomedicines.

To overcome the accumulation barrier, active targeting strategies represent a promising solution. Surface functionalization of nanocarriers with tumor-specific ligands (e.g., antibodies, peptides, biomimetic membranes) enables receptor-mediated active targeting (Saul et al., 2006; Shi et al., 2023; Spada and Gerber-Lemaire, 2025). Among these, cRGD peptides that present the Arg-Gly-Asp motif are especially attractive. They engage integrin  $\alpha_v\beta_3$ , a receptor markedly upregulated on both angiogenic endothelial cells and a broad spectrum of tumor cells. This dual specificity simultaneously amplifies tumor-selective enrichment and disrupts neovascularization, cooperatively curbing metastatic progression (Liu, 2009). Moreover, the constrained cyclic architecture endows cRGD with markedly higher affinity for  $\alpha_v\beta_3$  than its linear counterparts (Ye S. et al., 2020), a superiority we have previously validated in-house.

Simultaneously, incorporating stimulus-responsive bonds (pH-/ROS-/enzyme-cleavable bonds) into nanocarriers can endow NDDSs with spatiotemporal control (Yang et al., 2025; Du et al., 2010; Wei et al., 2022; Wei et al., 2021). Upon receptor-mediated internalization, these “smart” carriers rapidly release payloads under specific tumor microenvironmental cues, thereby resolving the

critical limitation of delayed intracellular drug availability. pH-sensitive liposomes have emerged as a promising area of interest. In normal human tissues and blood, the extracellular pH is typically maintained at 7.4. However, due to the high glycolytic activity of tumor cells, the extracellular pH in tumor tissues is often lower, ranging from 6.7 to 7.2. pH-sensitive liposomes are designed to respond to these subtle changes in the extracellular pH of the tumor microenvironment (Badparvar et al., 2023; Chen et al., 2013; Chen et al., 2012; Din et al., 2022; Liu et al., 2014; Charbe et al., 2020). The weakly acidic conditions of tumor tissues can trigger drug release from these liposomes. This targeted approach reduces drug exposure to normal tissues, minimizing the impact on healthy cells. Consequently, it has the potential to decrease the incidence and severity of adverse effects such as nausea, vomiting, diarrhea, and skin reactions.

Therefore, this study aims to develop a cRGD-modified, pH-sensitive, long-circulating liposome loaded with sorafenib (cRGD-pH-Lipo/Sor), which integrates prolonged circulation, active targeting, and pH-triggered drug release. This system is designed to enhance the delivery of chemotherapeutic drugs to hepatocellular carcinoma cells, thereby potentially improving anti-tumor efficacy. It may offer a novel strategy for targeted therapy in hepatocellular carcinoma.

## 2 Materials and methods

### 2.1 Materials

Egg yolk lecithin (EPC) was purchased from A.V.T. Pharmaceutical Co., Ltd. (Shanghai, China). Cholesterol was purchased from Sinopharm Chemical Reagent Co., Ltd. (Shanghai, China) and sorafenib was obtained from Shanghai Topscience Biotechnology Co., Ltd. (Shanghai, China). DSPE-PEG2K-cRGDyK, 1,2-Dioleoyl-sn-glycero-3-phosphoethanolamine (DOPE) was purchased from Xi'an Ruixi Biotechnology Co., Ltd. Cholesteryl hemisuccinate (CHEMS) was purchased from Avanti Research Co., Ltd. Coumarin 6 (C6) was purchased from Sigma (St. Louis, MO, United States). 1,1'-dioctadecyl-3,3,3',3'-tetramethylindotricarbocyanine iodide (DIR) was purchased from MedChemExpress Co., Ltd. (Monmouth Junction, NJ, United States). 5-(Dimethyl-thiazol-2-yl)-2,5-diphenyl-tetrazolium bromide (MTT) was purchased from Shanghai Sheng Er Biotechnology Co., Ltd. (Shanghai, China).

### 2.2 Preparation of liposomes

Liposomes were fabricated by the thin-film hydration technique. The formulation for conventional liposomes consisted of EPC and cholesterol at a mass ratio of 10:3. For cRGD-modified pH-sensitive liposomes (cRGD-pH-Lipo/Sor), the formulation was EPC, cholesterol, DOPE, CHEMS, and cRGD with a mass ratio of 10:3:4:4:0.4. The preparation process was as follows: First, all lipid materials were dissolved in 1 mL chloroform (CHCl<sub>3</sub>). A rotary evaporator (ZX-98; LOOYE, China) was employed to form a lipid film at 40 °C. After hydrating the thin film with 1 mL phosphate-buffered saline (PBS) at 40 °C for 30 min, the liposomal suspension was subjected to probe sonication in an ice bath (3 s of sonication

followed by 1 s of rest) at 300 W (20 kHz; Sonics and Materials, Inc.) for 3 min. The liposome suspension was centrifuged at 500 g for 3 min to pellet potential metal residues from the sonication probe. The entire supernatant was then carefully collected for subsequent characterization and experiments. Sorafenib-loaded liposomes were prepared by the same method, with the mass ratio of EPC to sorafenib set at 20:1.

Fluorescently labeled liposomes were prepared using the same materials and procedure as described above for the drug-loaded liposomes. The lipophilic dyes (Coumarin 6 (C6) for *in vitro* studies or DiR for *in vivo* imaging) were stably incorporated into the lipid bilayer by co-dissolving them with the lipid components in the organic phase during the initial film formation. Following hydration, any unencapsulated dye was removed by dialysis against PBS, guaranteeing that the observed fluorescence signal originated exclusively from the liposome-encapsulated dye.

### 2.3 Characterization of liposomes

The particle size and ζ-potential of all liposomes were detected by a dynamic light scattering (DLS) detector (Zetasizer, Nano-ZS; Malvern, UK). Liposomes were detected using transmission electron microscopy (TEM) (Tecnai G2 F20 S-Twin, FEI, United States). After being negatively stained with 2% phosphotungstic acid. High-performance liquid chromatography (HPLC; Agilent, United States) was used to determine the sorafenib encapsulation efficiency and drug-loading capacity (Li et al., 2015). A defined volume of the liposomal formulation was completely lysed with methanol. After appropriate dilution, the sorafenib concentration was quantified by HPLC and denoted as C<sub>total</sub>. An equal volume of the formulation was transferred to an ultrafiltration centrifugal tube with a molecular weight cutoff (MWCO) of 10 kD and centrifuged at 4,000×g for 40 min (Cence H1750R, 6 × 50 ml fixed-angle rotor). The drug concentration in the filtrate, representing unencapsulated sorafenib, was quantified by HPLC and denoted as C<sub>free</sub>. The encapsulation efficiency and drug loading capacity were calculated using the following equations:

$$EE\% = \frac{(C_{total} - C_{free})}{C_{total}} \times 100\%$$

$$DL\% = \frac{\text{encapsulated sorafenib (weight)}}{\text{liposome material (weight)}} \times 100\%$$

### 2.4 Stability of liposomes

Liposome stability was evaluated by monitoring hydrodynamic diameter changes by DLS over 1 week at 4 °C. Briefly, 1 mL liposomes were dispersed in 9 mL PBS, and the average size and polydispersity index (PDI) were measured by DLS every day for 7 days.

### 2.5 Release of liposomes

*In vitro* release of sorafenib was quantified by HPLC. One milliliter of liposome was loaded in dialysis bags [(MWCO) = 10K Da; 18 mm] and immediately immersed in 100 mL of release medium (PBS, pH 5.0, pH 6.8, pH 7.4) contained in

individual glass vessels, respectively. The vessels were shaken at 100 rpm, 37 °C. At predetermined intervals, 0.5 mL aliquots were withdrawn for analysis and replaced with an equal volume of fresh, pre-warmed medium to maintain sink conditions.

## 2.6 *In vitro* cellular uptake

To evaluate the targeting ability of the cRGD-pH-Lipo, coumarin 6 (C6) was encapsulated into liposomes to prepare C6-loaded fluorescent liposomes: C6-Lipo and cRGD-pH-Lipo/C6, with final C6 concentration of 25 ng/mL. Huh7 cells and HepG2 cells were respectively seeded into 12-well plates at a density of  $2 \times 10^5$  cells/well and cultured for 24 h. The medium was then replaced with fresh medium containing free C6 solution or the respective C6-loaded liposomes. After 4 h of incubation, cells were washed 3 times with ice-cold PBS and residual buffer carefully removed. The cells were fixed with 4% paraformaldehyde for 30 min at room temperature, stained with DAPI, and washed three times with cold PBS. Finally, fluorescence images were captured on an inverted fluorescence microscope (Carl Zeiss, Germany).

For the quantitative analysis, Huh7 cells and HepG2 cells were respectively seeded into 6-well plates at a density of  $5 \times 10^5$  cells/well and cultured for 24 h. Then, the medium was exchanged for fresh medium containing 10  $\mu$ M sorafenib solution, Sor-Lipo and cRGD-pH-Lipo/Sor. After 2 h of incubation, cells were washed three times with ice-cold PBS and residual buffer removed. Cells were lysed on ice by addition of 100  $\mu$ L lysis buffer followed by 30 min at 4 °C. Fifty microlitres of DMSO was added, and the lysed cells were collected into 1.5 mL tubes with a cell scraper. The cells were disrupted with an ultrasonic cell disruptor for 1–2 s, followed by the addition of 150  $\mu$ L of acetonitrile to precipitate proteins. After vortex mixing, the mixture was centrifuged at 12,000 rpm for 15 min. Twenty microlitres of the clear supernatant was injected onto HPLC to determine intracellular sorafenib levels.

## 2.7 Animals and tumor xenograft model

Four-to-six-week-old male BALB/c nude mice (weighing 18–22 g) were purchased from Shanghai SLAC Laboratory Animal Co, Ltd. and maintained under specific-pathogen-free facilities. To establish the tumor model, mice were inoculated subcutaneously into the right axilla with  $5 \times 10^6$  Huh7 cells suspended in 100  $\mu$ L PBS. Tumor growth was monitored, and experiments were initiated when the tumor volume reached approximately 100 mm<sup>3</sup>.

## 2.8 *In vivo* tissue distribution of liposomes in tumor-bearing mice

The *in vivo* tumor-targeting capacity of cRGD-pH-Lipo was evaluated in tumor xenograft model. When the volume of the tumor reached approximately 100 mm<sup>3</sup>, the mice randomly divided into two groups and injected intravenously (tail vein) with DiR-loaded conventional liposomes and cRGD-pH-Lipo. The fluorescence distribution were determined with an IVIS Spectrum imaging system (IVIS Spectrum; Caliper, United States) at predetermined time points (2, 4, 8, 12, and 24 h). At 24 h, the mice were sacrificed by cardiac perfusion with cold saline, and the tumors were excised and imaged *ex vivo* for final fluorescence confirmation.

## 2.9 Cell viability assay

The cytotoxicity of free sorafenib, Sor-Lipo and cRGD-pH-Lipo/Sor was evaluated in Huh7 cells and HepG2 cells using the CCK-8 assay. Huh7 cells and HepG2 cells were seeded in 96-well plates at  $5 \times 10^3$  cells per well and incubated for 24 h. Afterward, the medium was replaced with fresh medium containing serial dilutions of free sorafenib or the corresponding liposomal formulations (1  $\mu$ M, 2  $\mu$ M, 4  $\mu$ M, 8  $\mu$ M, 16  $\mu$ M) at identical sorafenib concentrations. Following 48 h of treatment, CCK-8 reagent (Beyotime, China) was added according to the manufacturer's instructions, and absorbance at 450 nm was measured on a microplate reader (Tecan, Switzerland).

## 2.10 *In vivo* antitumor effect

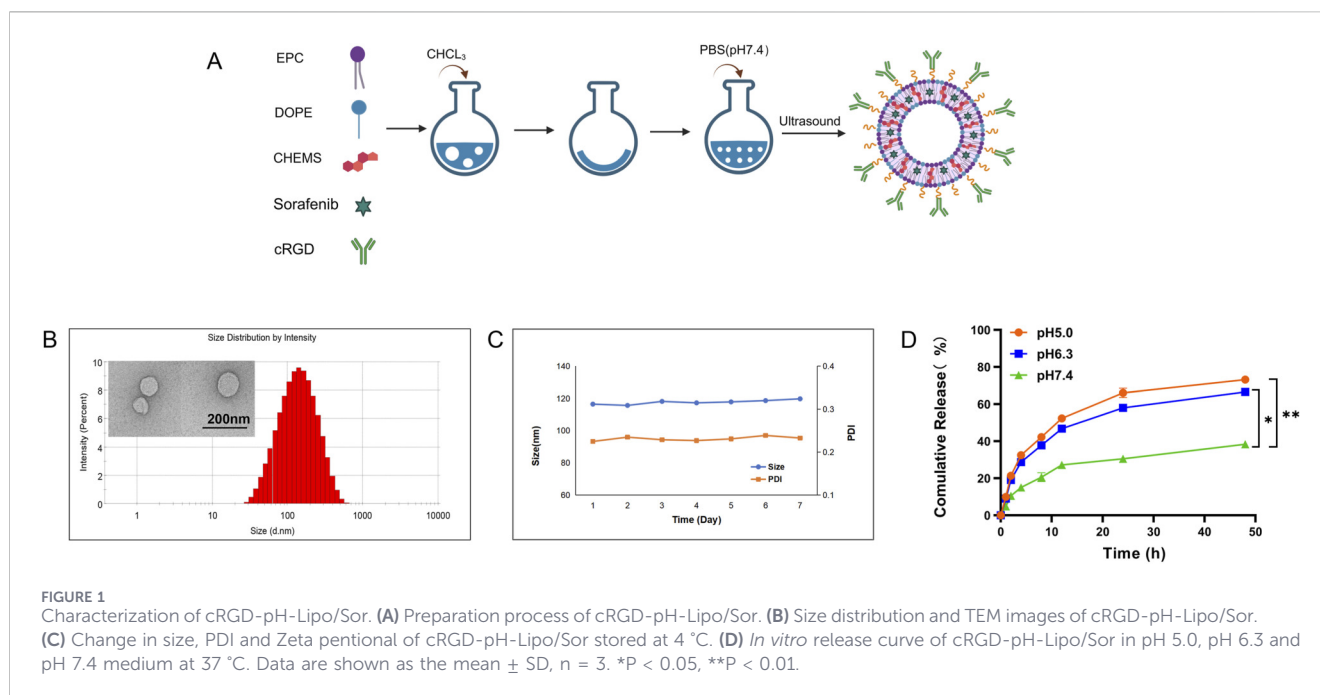
Animal experiments were approved by the Institutional Animal Care and Use Committee (IACUC) of Shanghai Jiaotong University (No.:A2024265-001). BALB/c nude (nu/nu) male mice (18–20 g) were inoculated subcutaneously into the right axilla with  $5 \times 10^6$  Huh7 cells suspended in 100  $\mu$ L PBS. 1 week later, when the tumor volume reached approximately 100 mm<sup>3</sup>, the mice were randomly divided into six groups with PBS, sorafenib (i.v., 10 mg/kg), Sor-Lipo (i.v. 10 mg/kg) and cRGD-pH-Lipo/Sor (i.v. 10 mg/kg) and treated every 2 days for 14 days. Sorafenib was dissolved in a mixture of Cremophor EL and ethanol (1:1, v/v). Tumor length (A) and width (B) were measured with digital calipers every 2 days, and the tumor volume was calculated using the formula  $A \times B^2/2$ . Body weight was recorded simultaneously. At the study end-point, mice were anesthetized and blood was collected. Tumors were immediately excised and weighed, the major organs were harvested in 10% formaldehyde solution for histopathological analysis.

## 2.11 Serum analysis

The blood of mice was collected and resting for 30 min at room temperature, and then centrifuged at 3000 g for 10 min at 4 °C to obtain serum. Serum alanine aminotransferase (ALT), creatinine (CREA) and blood urea nitrogen (BUN) levels were measured on a Cobas 8,000 modular analyzer (Roche).

## 2.12 Histopathology analysis

Formalin-fixed, paraffin-embedded tissue specimens were sectioned at 4  $\mu$ m thickness using a rotary microtome. After mounting on slides and drying, sections were dewaxed in xylene (two changes, 10 min each) and rehydrated through a graded ethanol series (100%, 95%, 70%, 5 min each). Subsequent hematoxylin and eosin (H&E) staining was performed as follows: nuclei were stained with Harris hematoxylin for 5–8 min, followed by brief differentiation in 1% acid ethanol and bluing in running tap water; cytoplasm was then counterstained with 0.5% eosin Y for 1–2 min. Finally, sections were dehydrated through ethanol, cleared in xylene, and mounted with resin medium. Stained sections were examined under a light microscope, and representative bright-field images were captured at  $\times 100$  magnification.



## 2.13 Statistical analysis

Data are presented as mean  $\pm$  standard deviation (SD) and were analyzed using GraphPad Prism 10.0 software (GraphPad Software, CA, United States). For multiple group comparisons, one-way analysis of variance (ANOVA) was performed followed by the Tukey's post-hoc test; comparisons between two groups were analyzed using the Student's t-test. Each experiment was conducted independently at least three times. P value < 0.05 was considered statistically significant.

## 3 Results

### 3.1 Characterization of cRGD-pH-Lipo/Sor

#### 3.1.1 Physicochemical characterization of cRGD-pH-Lipo/Sor

We prepared cRGD-pH-Lipo/Sor using the thin-film hydration method, with the detailed preparation process illustrated in Figure 1A. To characterize the properties of cRGD-pH-Lipo/Sor, particle size and zeta potential were measured using a Malvern particle size analyzer. Results showed that cRGD-pH-Lipo/Sor had an average particle size of  $116.73 \pm 1.07$  nm, a PDI of  $0.224 \pm 0.0017$ , and a zeta potential of  $-22.2 \pm 3.50$  mV (Figure 1B). The drug loading capacity of sorafenib in the liposomes was determined to be 2.16%, with an encapsulation efficiency of 84.06%. TEM imaging showed that the liposomes were spherical and uniform in size, indicating the successful construction of sorafenib liposomes with uniform morphology suitable for drug delivery. These results confirm that sorafenib can be effectively encapsulated into the liposomes.

#### 3.1.2 The stability of cRGD-pH-Lipo/Sor

Stability test was performed to qualify the capacity of preventing the drug from being damaged by external environment. As illustrated in Figure 1C, cRGD-pH-Lipo/Sor hold a stable particle size and PDI under storage condition.

#### 3.1.3 *In vitro* drug release of cRGD-pH-Lipo/Sor

The release profile of sorafenib over 48 h under pH 5.0, pH 6.3, and pH 7.4 conditions was evaluated via the dynamic membrane dialysis method, with its cumulative release percentage subsequently calculated. Specifically, the pH 7.4 environment was employed to mimic the normal physiological milieu, whereas pH 5.0 and pH 6.3 were designed to simulate the weakly acidic microenvironment characteristic of tumor regions. As shown in Figure 1D, the cumulative release rate of sorafenib from cRGD-pH-Lipo/Sor was 38.36% ( $\pm 1.94\%$ ) under pH 7.4, 66.59% ( $\pm 1.21\%$ ) under pH 6.3, while it reached 73.24% ( $\pm 2.03\%$ ) under pH 5.0. These results indicate that the carrier can release more sorafenib under acidic conditions (P < 0.001).

### 3.2 *In vitro* pharmacodynamic evaluation of cRGD-pH-Lipo/Sor

To evaluate the effect of cRGD-pH-Lipo/Sor on tumor cells *in vitro*, we assessed cytotoxicity using the CCK-8 assay. As shown in Figure 2, the blank liposomes (Blank-Lipo) showed no significant cytotoxicity at any concentration, with cell viability maintained above 90%. In contrast, within the concentration range of 4–16  $\mu$ M, the cRGD-pH-Lipo/Sor group induced a significant decrease in cell viability compared to the Blank-Lipo group. This result demonstrates that the observed cytotoxic effects were

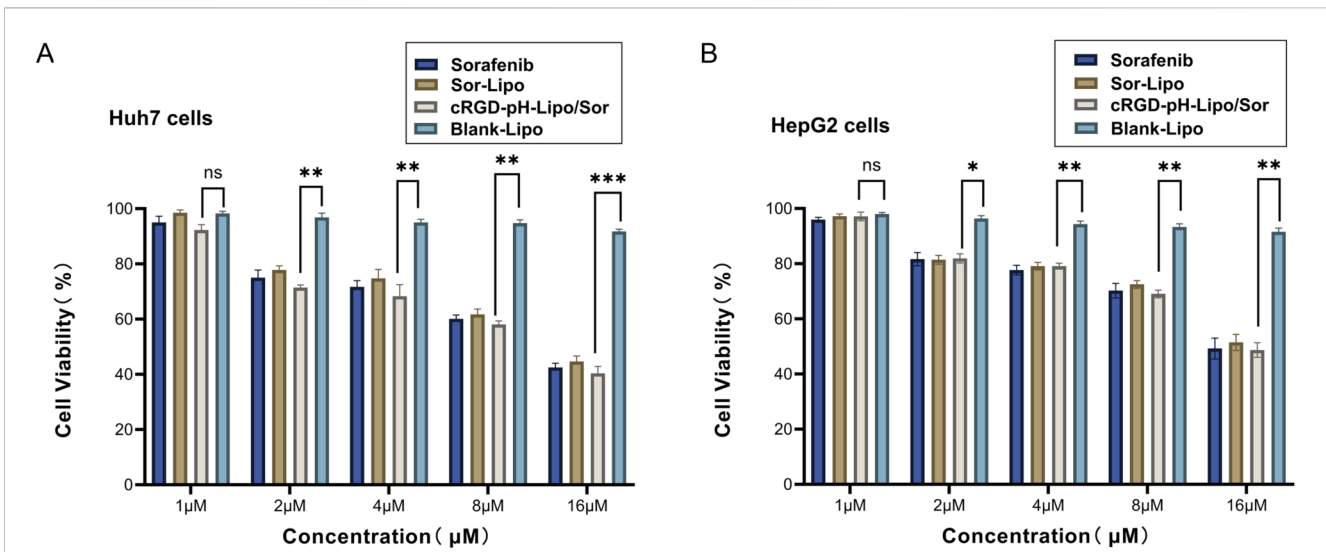


**FIGURE 2** *In vitro* cytotoxicities of cRGD-pH-Lipo/Sor against HepG2 cells and Huh7 cells following 24-h incubation. (A) HepG2 cells (B) Huh7 cells. Data are shown as the mean ± SD, n = 3. \*P < 0.05, P < 0.01, \*P < 0.001, ns means no significance. No statistically significant differences were observed among the free sorafenib, Sor-Lipo, and cRGD-pH-Lipo/Sor groups at any concentration.

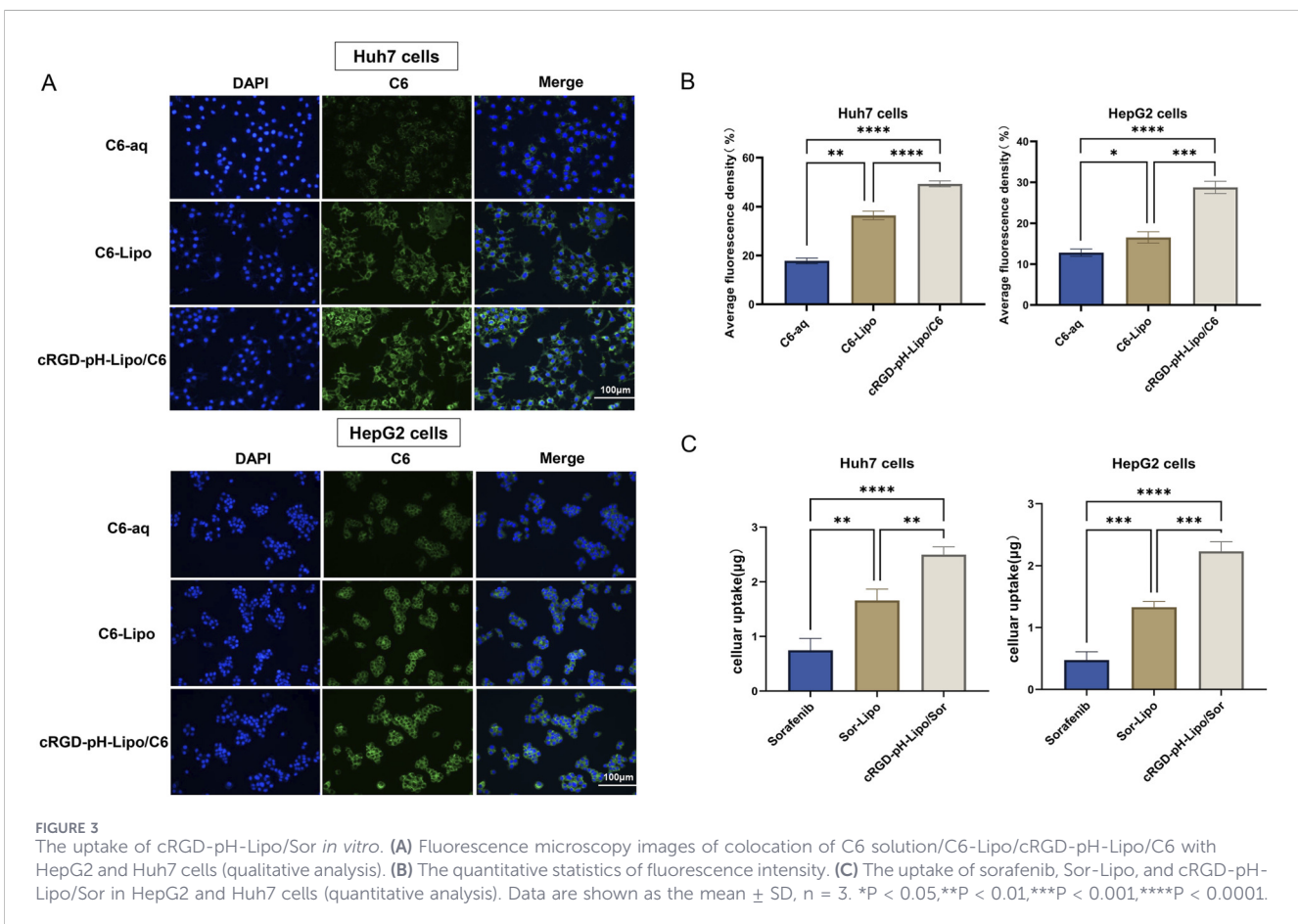


**FIGURE 3** The uptake of cRGD-pH-Lipo/Sor *in vitro*. (A) Fluorescence microscopy images of colocation of C6 solution/C6-Lipo/cRGD-pH-Lipo/C6 with HepG2 and Huh7 cells (qualitative analysis). (B) The quantitative statistics of fluorescence intensity. (C) The uptake of sorafenib, Sor-Lipo, and cRGD-pH-Lipo/Sor in HepG2 and Huh7 cells (quantitative analysis). Data are shown as the mean ± SD, n = 3. \*P < 0.05, \*\*P < 0.01, \*\*\*P < 0.001, \*\*\*\*P < 0.0001.

attributable to sorafenib rather than the lipid materials, confirming both the efficacy of the drug-loaded system and the safety of the delivery vehicle itself (P < 0.01). Meanwhile, no significant

differences in cytotoxicity were observed among the free drug, Sor-Lipo, and cRGD-pH-Lipo/Sor groups across the concentration range tested, indicating that cRGD-pH-Lipo/Sor

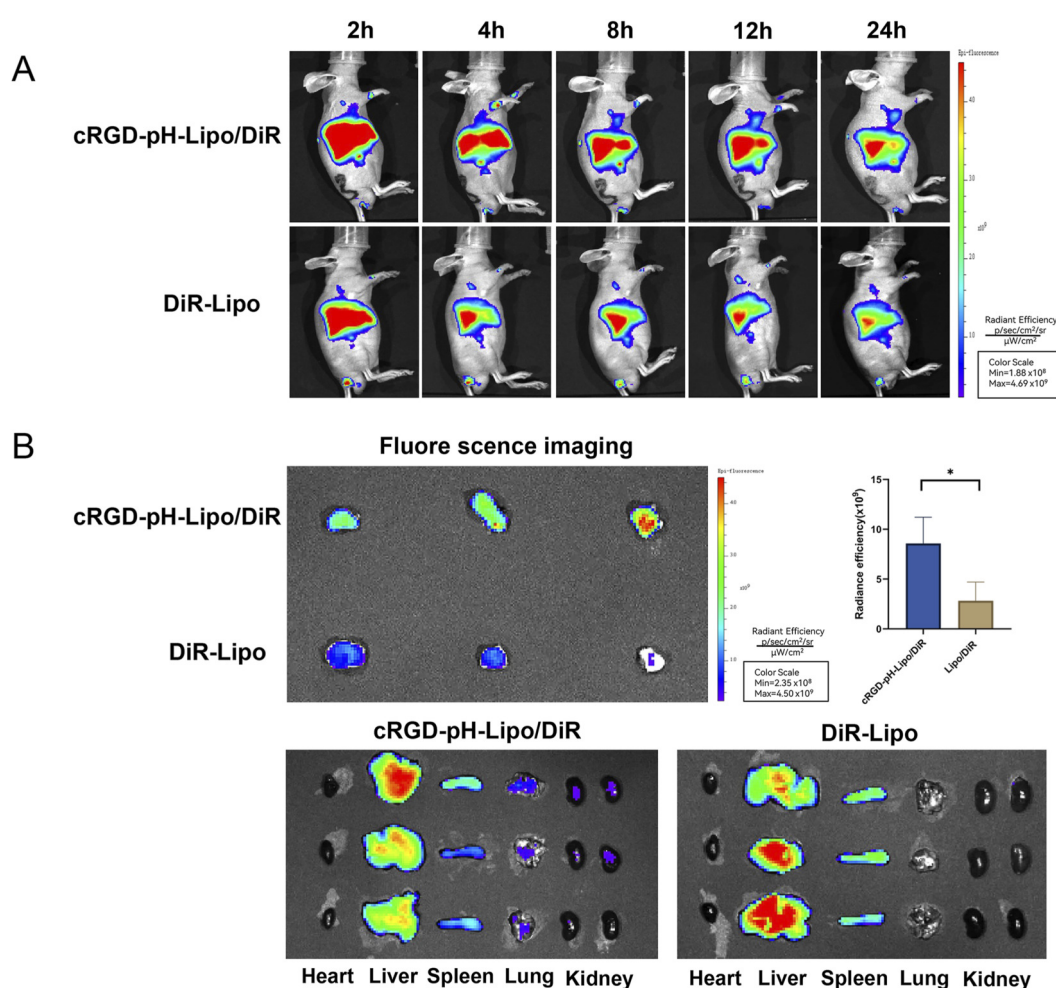


**FIGURE 4** Targeting effect of cRGD-pH-Lipo/Sor. (A) Fluorescence imaging of Huh7 tumor-bearing mice after administration of Sor-Lipo and cRGD-pH-Lipo/Sor at different time points. (B) Accumulation of Sor-Lipo and cRGD-pH-Lipo/Sor in mouse tumor tissues and various organs. Data are shown as the mean  $\pm$  SD, n = 3. \*P < 0.05.

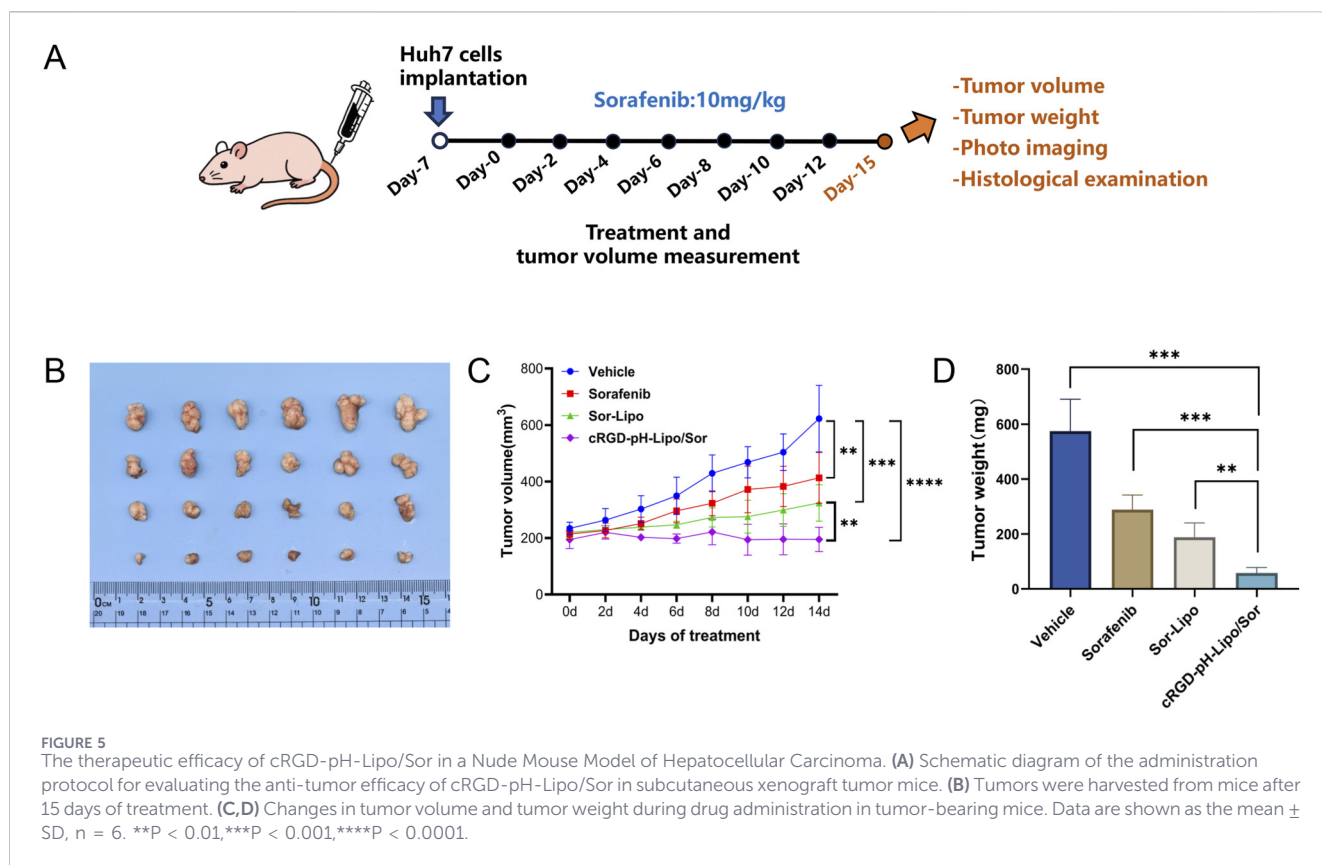
retains potent antitumor activity and that the delivery system does not diminish the inhibitory effect of sorafenib on cancer cells. Data are presented as mean  $\pm$  SD (n = 3). No statistically significant differences were observed among the free sorafenib, Sor-Lipo, and cRGD-pH-Lipo/Sor groups at any concentration.

### 3.3 *In vitro* cellular uptake of cRGD-pH-Lipo/Sor

The targeting efficacy of the liposomes was evaluated by assessing their cellular uptake in Huh7 and HepG2 cells using complementary qualitative and quantitative approaches. For qualitative analysis, as shown in Figure 3A, the cRGD-pH-Lipo/C6 group exhibited substantially stronger intracellular fluorescence in both cell lines compared to the free C6 solution and the non-targeted C6-Lipo groups. Fluorescence intensity was quantified using ImageJ software and expressed as average optical density. The results demonstrated a pronounced enhancement in uptake for the targeted formulation. Specifically, in Huh7 cells, the fluorescence intensity of cRGD-pH-Lipo/C6 was 2.77-fold and

1.35-fold higher than that of the free C6 solution and C6-Lipo, respectively. Similarly, in HepG2 cells, the intensity was 2.24-fold and 1.74-fold greater than the corresponding controls (Figure 3B). These data collectively confirm the superior cellular targeting and internalization efficiency of the cRGD-modified, pH-sensitive liposomes.

For quantitative analysis, as shown in Figure 3C, the cellular uptake of Sor-Lipo and cRGD-pH-Lipo/Sor in both Huh7 and HepG2 cells was significantly higher than that of free sorafenib, with cRGD-pH-Lipo/Sor exhibiting the highest uptake efficiency (P < 0.0001). Specifically, in Huh7 cells, the intracellular sorafenib concentration of cRGD-pH-Lipo/Sor was 3.44-fold and 1.51-fold higher than that of free sorafenib solution and Sor-Lipo, respectively. Similarly, in HepG2 cells, the intracellular sorafenib concentrations was 4.72-fold and 1.68-fold greater than the corresponding controls. Consistent with the fluorescence results, the cRGD-pH-Lipo/Sor group exhibited the optimal cellular uptake efficiency, further validating the enhanced internalization of the targeted, pH-sensitive delivery system (P < 0.0001).



### 3.4 Targeting study of liposomes

In order to investigate the targeting effect of cRGD-pH-Lipo on tumor sites, small animal live imaging technology was used to evaluate the distribution of liposomes in tumor-bearing mice. As shown in Figure 4A, after injecting cRGD-pH-Lipo/DiR into tumor-bearing mice, fluorescence signals can be detected at the tumor site, while common DiR-Lipo signals can hardly be detected at the tumor site, indicating that cRGD-pH-Lipo are more likely to accumulate at the tumor site and can more effectively and selectively deliver drugs to the tumor site. After injecting liposomes into the tail vein for 24 h, the fluorescence imaging and quantitative analysis of tumor tissues as shown in Figure 4B. The results showed that cRGD-pH-Lipo/DiR exhibited a much stronger fluorescent signal in tumor tissues compared to DiR-Lipo ( $p < 0.05$ ). These results indicate that cRGD-pH-Lipo has a superior ability to accumulate in tumor tissues, highlighting its potent tumor-targeting capability.

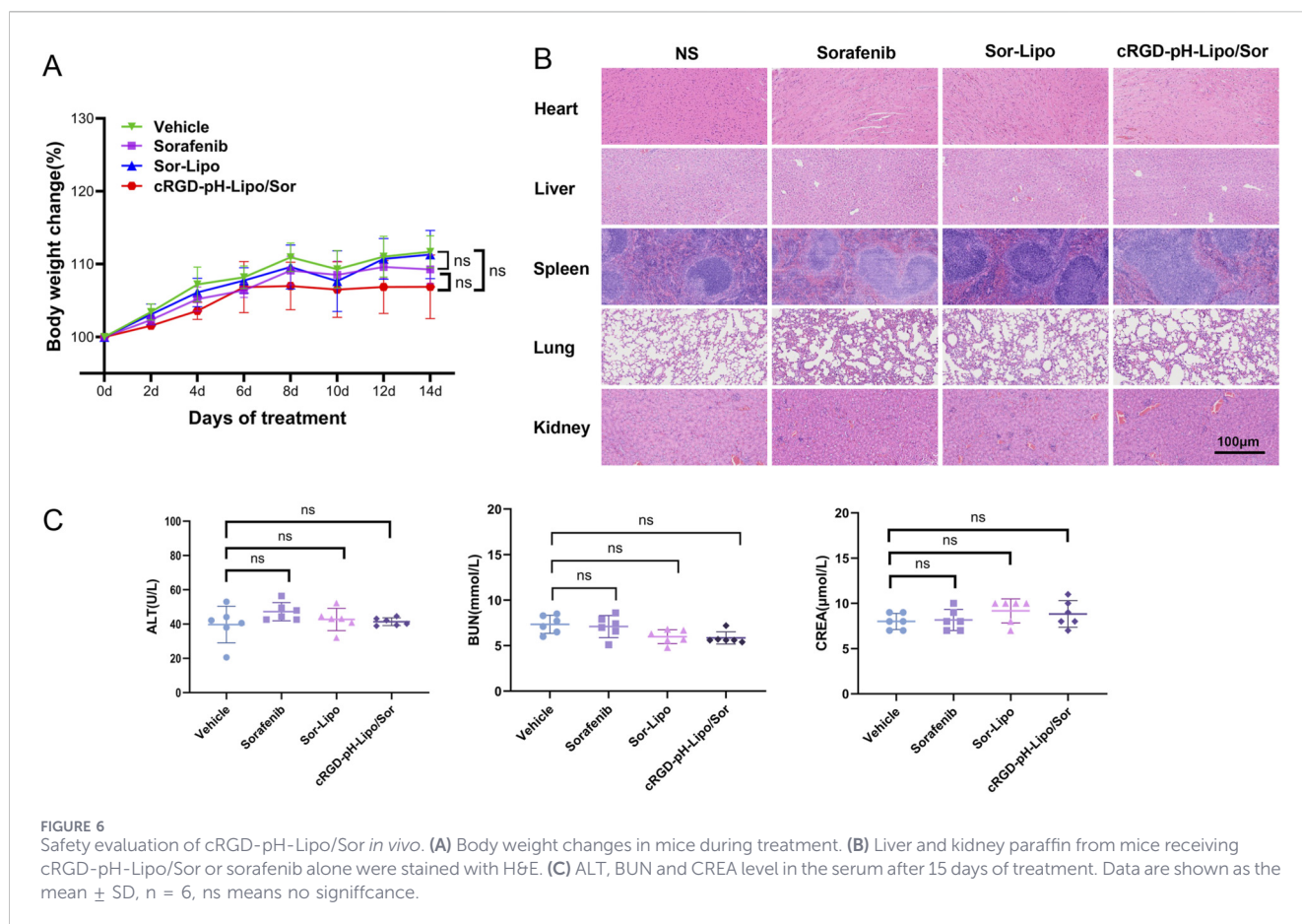
### 3.5 *In vivo* antitumor activity of cRGD-pH-Lipo/Sor

To further evaluate the anti-tumor efficacy of cRGD-pH-Lipo/Sor, we conducted animal efficacy experiments with tumor-bearing mice. A schematic diagram of the experimental procedure is shown in Figure 5A. As shown in Figure 5B, tumor volume in all groups exhibited a modest increase during the initial phase of the experiment. Beginning on the 4th day, the tumor growth curves of the control, sorafenib, and Sor-Lipo groups diverged noticeably, with tumors exhibiting a much steeper growth curve. At the study

endpoint, the sorafenib, Sor-Lipo, and cRGD-pH-Lipo/Sor groups all exhibited significant tumor growth inhibition compared to the control group, with the most pronounced effect observed in the cRGD-pH-Lipo/Sor group, which showed a significantly smaller tumor volume than all other groups (Figure 5C). As shown in Figure 4C, tumor weight in the cRGD-pH-Lipo/Sor group were markedly lighter than those in all other groups simultaneously ( $p < 0.001$ ). Specifically, relative to the cRGD-pH-Lipo/Sor group, tumor volumes in the control, free sorafenib, and Sor-Lipo groups were 3.19, 2.12, and 1.66 times greater, respectively, while tumor weights were 9.92, 4.99, and 3.24 times higher.

### 3.6 *In vivo* safety evaluation of cRGD-pH-Lipo/Sor

Throughout the entire experimental period, the body weight of mice in all groups remained relatively stable, with no statistically significant differences observed among the groups (Figure 6A). This indicates that at the administered dose, the toxicity of the targeted formulation was comparable to that of normal saline. Figure 6B shows H&E staining of the heart, liver, spleen, lung, and kidney tissues of mice. The results revealed no significant inflammatory lesions in any of these organs across the treatment groups compared with the control group, demonstrating the favorable safety profile of cRGD-pH-Lipo/Sor. ALT, BUN, and CREA in serum are key indicators for evaluating liver and kidney function, that provide a preliminary evaluate the safety of drugs. Biochemical analysis results (Figure 6C) showed that no statistically significant differences in serum ALT, BUN, or CREA levels among the groups compared with



the control. Combined with the results of pharmacodynamics, these findings indicate that the cRGD-pH-Lipo/Sor can not only significantly enhance the therapeutic efficacy of sorafenib, but also not cause obvious toxicological changes.

## 4 Discussion

The therapeutic landscape for advanced HCC has undergone remarkable transformation in recent years. The success of combination therapies integrating immune checkpoint inhibitors with antiangiogenic agents, particularly the atezolizumab-plus-bevacizumab regimen, has established a new first-line standard that demonstrates superior survival benefits over sorafenib monotherapy. Despite these advances, sorafenib retains a distinct clinical niche: it remains indispensable for patients with contraindications to immunotherapy, for second-line sequencing, and in resource-limited settings where cost or infrastructure precludes biologic combinations. Realizing its full potential therefore requires pharmacological strategies that overcome the native limitations of drugs.

The development of liposomal reformulation represents a significant pharmacological approach to addressing the native limitations of drugs. Native sorafenib is handicapped by poor aqueous solubility, extensive first-pass hepatic metabolism, and erratic oral absorption that together restrict absolute bioavailability to 38%–49%. To achieve therapeutic plasma levels, patients must tolerate high oral doses that precipitate hand–foot skin

reaction, diarrhoea, and fatigue toxicities that force dose reductions or discontinuation in up to one-third of cases. Liposomal nanoencapsulation offers a strategic solution to these challenges by fundamentally altering the drug's delivery paradigm. Through intravenous administration, liposomal formulations bypass the gastrointestinal absorption barriers and hepatic first-pass effect, thereby significantly improving systemic exposure.

In this work, to enhance the efficiency of sorafenib for hepatocarcinoma therapy, we developed a novel cRGD-modified and pH-sensitive liposomal formulation for sorafenib delivery (cRGD-pH-Lipo/Sor). The liposomes were prepared using the classical film dispersion method. As expected, the morphology of the liposomes was spherical, and the particle sizes of the different liposomes were about 100 nm. The *in vitro* targeting efficacy was assessed in two tumor cells including HepG2 and Huh7. The study showed cRGD-pH-Lipo/Sor had strong cellular uptake in both HepG2 and Huh7. The surface-conjugated cRGD peptides are designed to target the pathological overexpression of integrin  $\alpha_v\beta_3$  on HCC cells and tumor neovasculature, enabling active tumor targeting through receptor-mediated interactions. Our *in vivo* imaging results demonstrated enhanced tumor accumulation of cRGD-pH-Lipo compared to non-targeted liposomes, consistent with the established role of cRGD in promoting liposomal uptake in liver tumor models. This observation aligns with previous reports demonstrating that cRGD modification promotes liposomal accumulation in liver tumor models (Qiu et al., 2023; Zhou et al., 2022; Chen et al., 2021; Gajbhiye et al., 2019; Song et al., 2017).

The pH-sensitive component, incorporating CHEMS, represents another critical design feature to address the challenge of intracellular drug release. The slightly acidic tumor microenvironment (pH ~6.5–7.0) and the subsequent endolysosomal trafficking (pH 5.0–6.0) provide physiological triggers for controlled drug release. Our formulation demonstrated a pH-dependent release profile *in vitro*, with cumulative release rates of 73.24% at pH 5.0 and 66.59% at pH 6.3, compared to only 38.36% at physiological pH 7.4. This differential release behavior is designed to ensure preferential drug deployment within tumor tissue and intracellular compartments, thereby maximizing the local therapeutic concentration while minimizing off-target exposure. This characteristic is in agreement with the performance of other pH-sensitive liposomal systems documented in the literature.

To investigate the tumor-targeting capability of our designed liposomes, we employed small animal live imaging to assess their biodistribution in tumor-bearing mice. *In vivo* imaging results revealed a distinct fluorescence signal at the tumor site following the administration of cRGD-pH-Lipo/DiR, whereas minimal signal was detected for the non-targeted DiR-Lipo. This visual observation suggests a preferential accumulation of the cRGD-modified formulation at the tumor site. Quantitative analysis of excised tumors 24 h post-injection further corroborated this finding, demonstrating a significantly stronger fluorescent intensity for cRGD-pH-Lipo/DiR compared to the control liposomes ( $p < 0.05$ ). Collectively, these results confirm the superior tumor-targeting and localization efficiency conferred by the cRGD modification.

Subsequently, we evaluated the anti-tumor efficacy of the drug-loaded formulation, cRGD-pH-Lipo/Sor, in a xenograft model. Tumor growth curves indicated initial growth across all groups, followed by a marked divergence from day 4 onward. While tumors in the control, free sorafenib, and non-targeted Sor-Lipo groups exhibited accelerated growth, the cRGD-pH-Lipo/Sor group showed sustained and significant suppression. At the study endpoint, the tumors in the cRGD-pH-Lipo/Sor group were not only the smallest in volume but also the lightest in weight ( $p < 0.001$ ). Specifically, the final tumor volumes in the control, free sorafenib, and Sor-Lipo groups were 3.19-fold, 2.12-fold, and 1.66-fold larger, respectively, than that in the cRGD-pH-Lipo/Sor group. The differences in tumor weight were even more pronounced, with the control, free sorafenib, and Sor-Lipo groups showing 9.92-fold, 4.99-fold, and 3.24-fold higher weights, respectively. These compelling *in vivo* efficacy data strongly demonstrate that cRGD-pH-Lipo/Sor possesses significantly enhanced anti-tumor activity compared to both free sorafenib and the non-targeted liposomal formulation. This enhanced therapeutic outcome may be attributed to the synergistic combination of active tumor targeting and the microenvironment-responsive drug release profile engineered into our system.

An observation of note in this study is the discrepancy observed between *in vitro* cytotoxicity and *in vivo* antitumor efficacy. Although the targeted formulation, cRGD-pH-Lipo/Sor, demonstrated more pronounced tumor growth inhibition *in vivo*, its cytotoxic profile in cell culture models was comparable to that of non-targeted formulations or free sorafenib at equivalent nominal concentrations. This phenomenon can be

explained by the distinct contexts of the two experimental systems. In the cell culture environment, which lacks the physiological triggers necessary for release (e.g., acidic pH) and involves direct drug-cell contact. Although a greater number of liposomes are internalized, the kinetics of drug release from within the endolysosomal compartments may be slower or less synchronized compared to the immediate diffusion and action of free sorafenib. This likely results in reduced intracellular availability of the encapsulated drug at the measurement time point, leading to apparently similar cytotoxic effects. In contrast, the *in vivo* setting provides a sequence of biological conditions that can sequentially leverage the functional design of the cRGD-pH-Lipo/Sor system. First, prolonged circulation time and the enhanced permeability and retention effect facilitate accumulation within the tumor tissue. Subsequently, cRGD-mediated active targeting enhances specific cellular internalization. Finally, the locally acidic tumor microenvironment and the subsequent endolysosomal pathway following internalization are hypothesized to trigger the release of the encapsulated sorafenib, thereby increasing its effective local concentration at the target site. This multi-stage process, which cannot be replicated in simple monolayer cell culture, is likely the core reason for the superior therapeutic outcome observed in the animal model. This discrepancy displays that the realization of its therapeutic potential is dependent on the complete sequence of biological events—targeting, internalization, and triggered release. This finding aligns with the behavior of other stimulus-responsive nanocarriers and underscores the importance of *in vivo* models for evaluating their integrated functionality (Zhu and Torchilin, 2013).

This study has several limitations. First, the therapeutic efficacy was evaluated using a subcutaneous Huh7 xenograft model. While this model replicates high integrin  $\alpha_v\beta_3$  expression, it does not fully recapitulate the complex histopathology, desmoplastic stroma, and heterogeneous perfusion characteristics of human hepatocellular carcinoma. Employing orthotopic or patient-derived xenograft (PDX) models in the future would be valuable for validating the tumor penetration and efficacy of the formulation within a more clinically relevant microenvironment. Second, the evidence for active targeting, while supported by observations of enhanced tumor accumulation in imaging studies, requires further mechanistic validation. The precise receptor-mediated mechanism—including competitive binding to integrin  $\alpha_v\beta_3$  and the subsequent cellular internalization pathway—has not been conclusively established. Further investigations, such as competitive inhibition assays with free cRGD or the use of integrin  $\alpha_v\beta_3$  knockdown models, are necessary to definitively confirm the specificity of the targeting interaction. Moreover, while the enhanced therapeutic outcome is clearly demonstrated, the underlying molecular mechanisms—such as effects on key biomarkers of tumor proliferation and apoptosis—remain to be fully elucidated. Future studies will focus on this aspect to provide a deeper mechanistic understanding of the observed superiority. Third, regarding formulation characterization, the current stability study primarily focused on physical stability. A systematic evaluation that includes monitoring the

encapsulation efficiency over time is crucial for translational development. Additionally, although the lipid components used are generally recognized as biocompatible and no carrier-related toxicity was observed *in vivo*, a complete safety assessment including empty liposomes remains an important aspect of future preclinical studies. Finally, the efficacy of this delivery system in models of acquired sorafenib resistance remains unexplored and represents a critical direction for future research to define its potential utility in treatment-resistant settings.

Despite these limitations, cRGD-pH-Lipo/Sor offers potential beyond single-agent application. Achieving higher intratumoral concentrations with reduced systemic exposure provides a rationale for combination strategies, particularly with immune checkpoint inhibitors. Sorafenib modulates the tumor immune microenvironment through effects on myeloid-derived suppressor cells and tumor-associated macrophages; local enhancement of these immunomodulatory effects via targeted delivery may help overcome resistance and improve immunotherapy response rates.

In conclusion, cRGD-pH-Lipo/Sor represents a rational nanomedicine approach to address key pharmacological limitations of sorafenib in HCC. Integration of active targeting and stimuli-responsive release demonstrates feasible improvement in tumor-specific delivery. Future work addressing mechanistic validation of targeting, detailed pharmacokinetics, and evaluation in advanced or resistant models will be essential to clarify the translational potential of this system.

## 5 Conclusion

In summary, we successfully developed a cRGD-modified, pH-sensitive liposomal formulation for the delivery of sorafenib. This system was designed to integrate prolonged circulation, active tumor targeting, and acidic microenvironment-responsive drug release, thereby addressing several key pharmacological limitations of native sorafenib. *In vitro* and *in vivo* studies demonstrated that cRGD-pH-Lipo/Sor exhibits favorable physicochemical characteristics and a pH-dependent drug release profile. The formulation promotes enhanced cellular uptake in tumor cells, facilitates intracellular drug release under acidic conditions. In tumor-bearing mice, cRGD-pH-Lipo/Sor showed improved accumulation at the tumor site and superior antitumor activity compared to free sorafenib and non-targeted liposomal controls. Notably, this enhanced efficacy was not accompanied by increased systemic toxicity, supporting its favorable safety profile.

Collectively, these findings indicate that cRGD-pH-Lipo/Sor constitutes a rational and effective nanomedicine-based strategy for targeted sorafenib delivery in hepatocellular carcinoma, warranting further investigation toward potential clinical translation.

## Data availability statement

The raw data supporting the conclusions of this article will be made available by the authors, without undue reservation.

## Ethics statement

The animal experiments were approved by the Institutional Animal Care and Use Committee (IACUC) of Shanghai Jiaotong University. The study was conducted in accordance with the local legislation and institutional requirements.

## Author contributions

XY: Conceptualization, Data curation, Formal Analysis, Funding acquisition, Methodology, Software, Writing – original draft, Writing – review and editing. GS: Conceptualization, Project administration, Supervision, Writing – review and editing. XZ: Data curation, Formal Analysis, Methodology, Writing – review and editing. QL: Investigation, Validation, Writing – review and editing. JL: Data curation, Formal Analysis, Writing – review and editing.

## Funding

The author(s) declared that financial support was received for this work and/or its publication. This study was sponsored by Health Profession Clinical Research Funds of Shanghai Municipal Health Commission (20214Y0344) and Key Medical Specialty funded by Health Commission of Minhang District (2025MWTZB02).

## Conflict of interest

The author(s) declared that this work was conducted in the absence of any commercial or financial relationships that could be construed as a potential conflict of interest.

## Generative AI statement

The author(s) declared that generative AI was used in the creation of this manuscript. During the preparation of this work, the authors used generative AI tools (specifically, [Deepseek/Kimi-k2]) for the purpose of language polishing, grammar checking, and improving readability. After using these tools, the authors reviewed and edited the content as needed.

Any alternative text (alt text) provided alongside figures in this article has been generated by Frontiers with the support of artificial intelligence and reasonable efforts have been made to ensure accuracy, including review by the authors wherever possible. If you identify any issues, please contact us.

## Publisher's note

All claims expressed in this article are solely those of the authors and do not necessarily represent those of their affiliated organizations, or those of the publisher, the editors and the reviewers. Any product that may be evaluated in this article, or claim that may be made by its manufacturer, is not guaranteed or endorsed by the publisher.

## References

- Abu Lila, A. S., and Ishida, T. (2017). Liposomal delivery systems: design optimization and current applications. *Biol. Pharm. Bull.* 40 (1), 1–10. doi:10.1248/bpb.b16-00624
- Allen, T. M., and Cullis, P. R. (2013). Liposomal drug delivery systems: from concept to clinical applications. *Adv. Drug Deliv. Rev.* 65 (1), 36–48. doi:10.1016/j.addr.2012.09.037
- Badparvar, F., Marjani, A. P., Salehi, R., and Ramezani, F. (2023). pH/redox responsive size-switchable intelligent nanovehicle for tumor microenvironment targeted DOX release. *Sci. Rep.* 13 (1), 22475. doi:10.1038/s41598-023-49446-x
- Barua, S., and Mitragotri, S. (2014). Challenges associated with penetration of nanoparticles across cell and tissue barriers: a review of current status and future prospects. *Nano Today* 9 (2), 223–243. doi:10.1016/j.nantod.2014.04.008
- Cappuyns, S., Piqué-Gili, M., Esteban-Fabro, R., Philips, G., Balaseviciute, U., Pinyol, R., et al. (2025). Single-cell RNA sequencing-derived signatures define response patterns to atezolizumab + bevacizumab in advanced hepatocellular carcinoma. *J. Hepatol.* 82 (6), 1036–1049. doi:10.1016/j.jhep.2024.12.016
- Chan, Y. T., Zhang, C., Wu, J., Lu, P., Xu, L., Yuan, H., et al. (2024). Biomarkers for diagnosis and therapeutic options in hepatocellular carcinoma. *Mol. Cancer* 23 (1), 189. doi:10.1186/s12943-024-02101-z
- Charbe, N. B., Amnerkar, N. D., Ramesh, B., Tambuwala, M. M., Bakshi, H. A., Aljabali, A. A. A., et al. (2020). Small interfering RNA for cancer treatment: overcoming hurdles in delivery. *Acta Pharm. Sin. B* 10 (11), 2075–2109. doi:10.1016/j.apsb.2020.10.005
- Chen, D., Sun, K., Mu, H., Tang, M., Liang, R., Wang, A., et al. (2012). pH and temperature dual-sensitive liposome gel based on novel cleavable mPEG-Hz-CHEMS polymeric vaginal delivery system. *Int. J. Nanomedicine* 7, 2621–2630. doi:10.2147/ijn.S31757
- Chen, Y., Sun, J., Lu, Y., Tao, C., Huang, J., Zhang, H., et al. (2013). Complexes containing cationic and anionic pH-sensitive liposomes: comparative study of factors influencing plasmid DNA gene delivery to tumors. *Int. J. Nanomedicine* 8, 1573–1593. doi:10.2147/ijn.S42800
- Chen, L., Liu, Y., and Wang, W. L. K. (2021). Effect of integrin receptor-targeted liposomal paclitaxel for hepatocellular carcinoma targeting and therapy. *Oncol. Lett.* 21 (5), 350. doi:10.3892/ol.2021.12611
- Cheng, A. L., Kang, Y. K., Chen, Z., Tsao, C. J., Qin, S., Kim, J. S., et al. (2009). Efficacy and safety of sorafenib in patients in the Asia-Pacific region with advanced hepatocellular carcinoma: a phase III randomised, double-blind, placebo-controlled trial. *Lancet Oncol.* 10 (1), 25–34. doi:10.1016/s1470-2045(08)70285-7
- Ding, H., Tan, P., Fu, S., Tian, X., Zhang, H., Ma, X., et al. (2022). Preparation and application of pH-responsive drug delivery systems. *J. Control Release* 348, 206–238. doi:10.1016/j.jconrel.2022.05.056
- Du, J. Z., Sun, T. M., Song, W. J., Wu, J., and Wang, J. (2010). A tumor-acidity-activated charge-conversional nanogel as an intelligent vehicle for promoted tumoral-cell uptake and drug delivery. *Angew. Chem. Int. Ed. Engl.* 49 (21), 3621–3626. doi:10.1002/anie.200907210
- ElZayat, E. M., Hassan, N. M., Mahmoud, R., Ibrahim, E., and Hassan, N. (2025). MOF enhances the sensitivity and selectivity of sorafenib as an anticancer drug against hepatocellular carcinoma and colorectal cancer *in vitro*. *Sci. Rep.* 15 (1), 32596. doi:10.1038/s41598-025-16803-x
- Escudier, B., Worden, F., and Kudo, M. (2019). Sorafenib: key lessons from over 10 years of experience. *Expert Rev. Anticancer Ther.* 19 (2), 177–189. doi:10.1080/14737140.2019.1559058
- Farjadian, F., Ghasemi, A., Gohari, O., Roointan, A., Karimi, M., and Hamblin, M. R. (2019). Nanopharmaceuticals and nanomedicines currently on the market: challenges and opportunities. *Nanomedicine (Lond.)* 14 (1), 93–126. doi:10.2217/nmm-2018-0120
- Finn, R. S., Qin, S., Ikeda, M., Galle, P. R., Ducreux, M., Kim, T. Y., et al. (2020). Atezolizumab plus bevacizumab in unresectable hepatocellular carcinoma. *N. Engl. J. Med.* 382 (20), 1894–1905. doi:10.1056/NEJMoa1915745
- Gajbhiye, K. R., Gajbhiye, V., Siddiqui, I. A., and Gajbhiye, J. M. (2019). cRGD functionalised nanocarriers for targeted delivery of bioactives. *J. Drug Target* 27 (2), 111–124. doi:10.1080/1061186x.2018.1473409
- Gordan, J. D., Kennedy, E. B., Abou-Alfa, G. K., Beal, E., Finn, R. S., Gade, T. P., et al. (2024). Systemic therapy for advanced hepatocellular carcinoma: ASCO guideline update. *J. Clin. Oncol.* 42 (15), 1830–1850. doi:10.1200/jco.23.027459
- He, H., Lu, Y., Qi, J., Zhu, Q., Chen, Z., and Wu, W. (2019). Adapting liposomes for oral drug delivery. *Acta Pharm. Sin. B* 9 (1), 36–48. doi:10.1016/j.apsb.2018.06.005
- Hossen, S., Hossain, M. K., Basher, M. K., Mia, M. N. H., Rahman, M. T., and Uddin, M. J. (2019). Smart nanocarrier-based drug delivery systems for cancer therapy and toxicity studies: a review. *J. Adv. Res.* 15, 1–18. doi:10.1016/j.jare.2018.06.005
- Lee, Y., and Thompson, D. H. (2017). Stimuli-responsive liposomes for drug delivery. *Wiley Interdiscip. Rev. Nanomed Nanobiotechnol* 9 (5). doi:10.1002/wnan.1450
- Li, Y. J., Dong, M., Kong, F. M., and Zhou, J. P. (2015). Folate-decorated anticancer drug and magnetic nanoparticles encapsulated polymeric carrier for liver cancer therapeutics. *Int. J. Pharm.* 489 (1–2), 83–90. doi:10.1016/j.ijpharm
- Liu, S. (2009). Radiolabeled cyclic RGD peptides as integrin alpha(v)beta(3)-targeted radiotracers: maximizing binding affinity via bivalency. *Bioconjug Chem.* 20 (12), 2199–2213. doi:10.1021/bc900167c
- Liu, J., Huang, Y., Kumar, A., Tan, A., Jin, S., Mozhi, A., et al. (2014). pH-sensitive nano-systems for drug delivery in cancer therapy. *Biotechnol. Adv.* 32 (4), 693–710. doi:10.1016/j.biotechadv.2013.11.009
- Liu, C., Chen, Z., Chen, Y., Lu, J., Li, Y., Wang, S., et al. (2016). Improving oral bioavailability of sorafenib by optimizing the “Spring” and “Parachute” based on molecular interaction mechanisms. *Mol. Pharm.* 13 (2), 599–608. doi:10.1021/acs.molpharmaceut.5b00837
- Llovet, J. M., Ricci, S., Mazzaferro, V., Hilgard, P., Gane, E., Blanc, J. F., et al. (2008). Sorafenib in advanced hepatocellular carcinoma. *N. Engl. J. Med.* 359 (4), 378–390. doi:10.1056/NEJMoa0708857
- Llovet, J. M., Montal, R., and Sia, D. F. R. S. (2018). Molecular therapies and precision medicine for hepatocellular carcinoma. *Nat. Rev. Clin. Oncol.* 15 (10), 599–616. doi:10.1038/s41571-018-0073-4
- Marrero, J. A., Kudo, M., Venook, A. P., Ye, S. L., Bronowicki, J. P., Chen, X. P., et al. (2016). Observational registry of sorafenib use in clinical practice across child-pugh subgroups: the GIDEON study. *J. Hepatol.* 65 (6), 1140–1147. doi:10.1016/j.jhep.2016.07.020
- Perche, F., and Torchilin, V. P. (2013). Recent trends in multifunctional liposomal nanocarriers for enhanced tumor targeting. *J. Drug Deliv.* 2013, 705265. doi:10.1155/2013/705265
- Qiu, M., Wang, J., Bai, J., Li, X., Tian, C., Liu, Z., et al. (2023). Dual-ligand-functionalized liposomes based on glycyrrhetic acid and cRGD for hepatocellular carcinoma targeting and therapy. *Mol. Pharm.* 20 (4), 1951–1963. doi:10.1021/acs.molpharmaceut.2c00842
- Sung, H., Ferlay, J., Siegel, R. L., Laversanne, M., Soerjomataram, I., Jemal, A., et al. (2021). Global cancer statistics 2020: GLOBOCAN estimates of incidence and mortality worldwide for 36 cancers in 185 countries. *CA Cancer J. Clin.* 71 (3), 209–249. doi:10.3322/caac.21660
- Saul, J. M., Annapragada, A. V., and Bellamkonda, R. V. (2006). A dual-ligand approach for enhancing targeting selectivity of therapeutic nanocarriers. *J. Control Release* 114 (3), 277–287. doi:10.1016/j.jconrel.2006.05.028
- Shi, P., Cheng, Z., Zhao, K., Chen, Y., Zhang, A., Gan, W., et al. (2023). Active targeting schemes for nano-drug delivery systems in osteosarcoma therapeutics. *J. Nanobiotechnology* 21 (1), 103. doi:10.1186/s12951-023-01826-1
- Shukla, S. K., Goyal, M., Kanabar, D. D., Ayeahunie, S., Deore, B., Sanhueza, C. A., et al. (2024). Exploring the enhanced stability and therapeutic efficacy of sorafenib-cyclodextrin inclusion complex. *J. Mol. Liq.* 401, 124701. doi:10.1016/j.molliq.2024.124701
- Song, Z., Lin, Y., Zhang, X., Feng, C., Lu, Y., Gao, Y., et al. (2017). Cyclic RGD peptide-modified liposomal drug delivery system for targeted oral apatinib administration: enhanced cellular uptake and improved therapeutic effects. *Int. J. Nanomedicine* 12, 1941–1958. doi:10.2147/ijn.S125573
- Spada, A., and Gerber-Lemaire, S. (2025). Surface functionalization of nanocarriers with Anti-EGFR ligands for cancer active targeting. *Nanomater. (Basel)* 15 (3), 158. doi:10.3390/nano15030158
- Tang, W., Chen, Z., Zhang, W., Cheng, Y., Zhang, B., Wu, F., et al. (2020). The mechanisms of sorafenib resistance in hepatocellular carcinoma: theoretical basis and therapeutic aspects. *Signal Transduct. Target Ther.* 5 (1), 87. doi:10.1038/s41392-020-0187-x
- Vogel, A., Qin, S., Kudo, M., Su, Y., Hudgens, S., Yamashita, T., et al. (2021). Lenvatinib versus sorafenib for first-line treatment of unresectable hepatocellular carcinoma: patient-reported outcomes from a randomised, open-label, non-inferiority, phase 3 trial. *Lancet Gastroenterol. Hepatol.* 6 (8), 649–658. doi:10.1016/s2468-1253(21)00110-2
- Vogel, A., Meyer, T., Sapisochin, G., Salem, R., and Saborowski, A. (2022). Hepatocellular carcinoma. *Lancet* 400 (10360), 1345–1362. doi:10.1016/s0140-6736(22)01200-4
- Wei, X., Song, M., Li, W., Huang, J., Yang, G., and Wang, Y. (2021). Multifunctional nanoplateforms co-delivering combinatorial dual-drug for eliminating cancer multidrug resistance. *Theranostics* 11 (13), 6334–6354. doi:10.7150/thno.59342
- Wei, X., Song, M., Jiang, G., Liang, M., Chen, C., Yang, Z., et al. (2022). Progress in advanced nanotherapeutics for enhanced photodynamic immunotherapy of tumor. *Theranostics* 12 (12), 5272–5298. doi:10.7150/thno.73566
- Xia, S., Pan, Y., Liang, Y., and Xu, J. C. X. (2020). The microenvironmental and metabolic aspects of sorafenib resistance in hepatocellular carcinoma. *EBioMedicine* 51, 102610. doi:10.1016/j.ebiom.2019.102610
- Xie, E., Yeo, Y. H., Scheiner, B., Zhang, Y., Hiraoka, A., Tantai, X., et al. (2023). Immune checkpoint inhibitors for child-pugh class B advanced hepatocellular carcinoma: a

systematic review and meta-analysis. *JAMA Oncol.* 9 (10), 1423–1431. doi:10.1001/jamaoncol.2023.3284

Yang, J., des Rieux, A., and Malfanti, A. (2025). Stimuli-responsive nanomedicines for the treatment of non-cancer related inflammatory diseases. *ACS Nano* 19 (16), 15189–15219. doi:10.1021/acsnano.5c00700

Ye, H., Zhou, L., Jin, H., Chen, Y., Cheng, D., and Jiang, Y. (2020). Sorafenib-loaded long-circulating nanoliposomes for liver cancer therapy. *Biomed. Res. Int.* 2020, 1351046. doi:10.1155/2020/1351046

Ye, S., Liu, Y., Lu, Y., Ji, Y., Mei, L., Yang, M., et al. (2020). Cyclic RGD functionalized liposomes targeted to activated platelets for thrombosis dual-mode magnetic resonance imaging. *J. Mater. Chem. B* 8 (3), 447–453. doi:10.1039/c9tb01834d

Zhou, R., Zhang, M., He, J., Liu, J., Sun, X., and Ni, P. (2022). Functional cRGD-Conjugated polymer prodrug for targeted drug delivery to liver cancer cells. *ACS Omega* 7 (24), 21325–21336. doi:10.1021/acsomega.2c02683

Zhu, L., and Torchilin, V. P. (2013). Stimulus-responsive nanopreparations for tumor targeting. *Integr. Biol. (Camb)*. 5 (1), 96–107. doi:10.1039/c2ib20135f